Chapter 3

Modelling of He Diagnostic Beams

3.1 Introduction

During the last years, fast lithium beam diagnostics has become a well established tool for determining electron density profiles (Li-IXS, Li impact excitation spectroscopy [2, 3]) and impurity ion temperature- and density profiles (Li-CXS, Li charge-exchange spectroscopy [2, 79]) of fusion edge plasmas. For such diagnostic measurements, a fast Li beam of several 10 keV energy and some mA equivalent current is injected into the fusion plasma. The electron spin configuration of neutral Li is doublet only, and the ionization energy is 5.39 eV. The excitation- and ionization rate coefficients of Li show only a weak dependence on the temperature in the temperature region of diagnostic interest (see figure 3.1), and furthermore, the ratio of these rate coefficients is almost independent of the electron temperature. Hence, the population densities of the ground state and excited levels can simply be determined by measuring one Li emission line along the beam path and solving the balance equations for all states involved. The model includes levels for up to n = 4, whereas higher levels can be neglected. The observed Li line is 670 nm (2p→2s) as the most intense one. The derived information about the population densities of ground state and excited states makes it possible to reconstruct the electron density profile by inverting the balance equations (Li-IXS [29, 80, 81]). In Li-CXS measurements the injected Li atoms act as electron donors for the impurity ions. Generally, the electrons are captured into excited states of the ions which subsequently emit photons. From the intensities of these lines the ion densities can be deduced. The full width at half maximum of the emission lines gives access to the ion temperature [30].

The atomic features of neutral He are somewhat different from neutral Li. Helium occurs

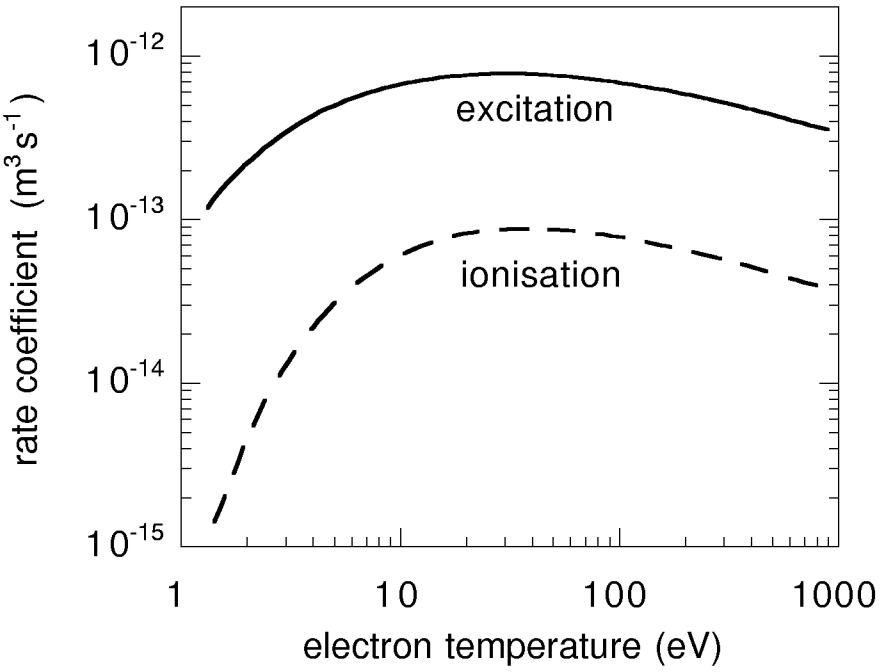

Figure 3.1: LiI rate coefficients for excitation from ground state to the lowest excited state (2p, solid line) and for ionization of the ground state (dashed line) [82].

in two different spin systems, namely singlet (i.e., $S = \sum s_i = 0$, the spins of the two electrons are antiparallel) and triplet (i.e., $S = \sum s_i = 1$, the two electron spins are parallel). Furthermore, two excited He states are metastable (the binding-energy level diagram of He is shown in figure 3.2). Helium has the largest ground state ionization energy of all atoms, 24.6 eV. Hence, a He beam should penetrate into a plasma much further than a Li beam of the same energy. Consequently the diagnostic region could be extended into the plasma core by using a He beam instead of a Li beam. The ionization energy of the two metastable levels 2^1S and 2^3S is 3.97 eV and 4.77 eV, respectively, which is in the order of the ionization energy of the Li ground state. This fact suggests using of He beams for charge-exchange spectroscopy also, where the metastable levels should act as electron donors for the impurity ions. This feature raises the question whether a high initial metastable fraction in the beam would be favourable.

An additional advantage of He beams compared with Li beams is based on the fact that He occurs in two different spin systems. The triplet system can only be populated by spin-changing processes, i.e. electron collisions, whereas the singlet metastable and other excited states are mainly populated by spin-conserving processes from the ground state. The different behaviour of cross sections for spin-changing and spin-conserving collisions leads to a rather different temperature dependence of the excitation rate coefficients, see

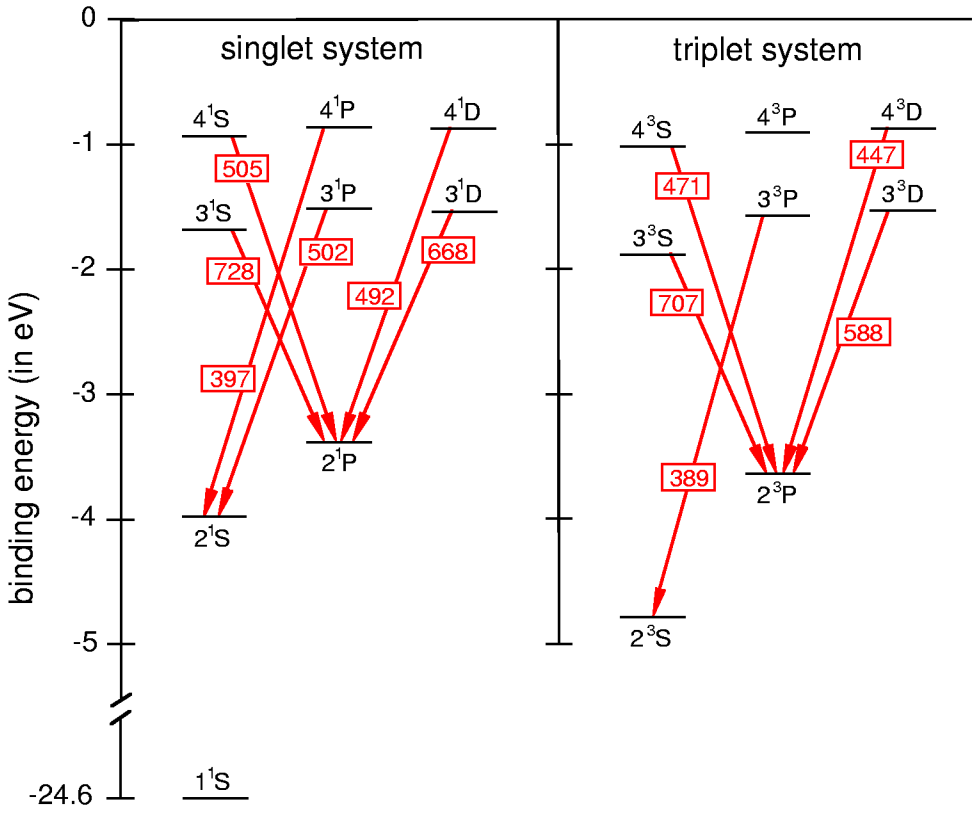

Figure 3.2: Binding energy level diagram of He including the states with n $\leq$ 4 and l $\leq$ 3, and optical lines of present diagnostic interest.

figures 3.3 to 3.5. For the electron-impact excitation out of the ground state (figure 3.3) the difference between spin-conserving and spin-changing processes becomes apparent for electron temperatures exceeding 20 eV. The spin-conserving processes have a rather flat maximum at several 100 eV and can be considered as almost constant in the region between 50 eV and 10 keV. The maximum of the rate coefficients for spin-changing collisions out of the ground state is at about 30 eV and at higher energies they decrease approximately with T_e^{-2}. In figures 3.4 and 3.5 excitation rate coefficients are shown out of the metastable triplet and singlet state, respectively. As expected, all the maxima are displaced toward lower temperatures compared with ground state excitation. The curves for the spin-conserving processes out of metastable states are much flatter than those out of the ground state, i.e. the temperature dependence is much smaller than for excitation out of the ground state, especially in the low temperature region. The spin-changing rate coefficients start to fall on the low temperature side at about 10 eV. In figure 3.4 also the excitation from the metastable triplet to the metastable singlet state is shown. It is about 10 times larger than excitation into the $(n = 3)$-singlet levels.

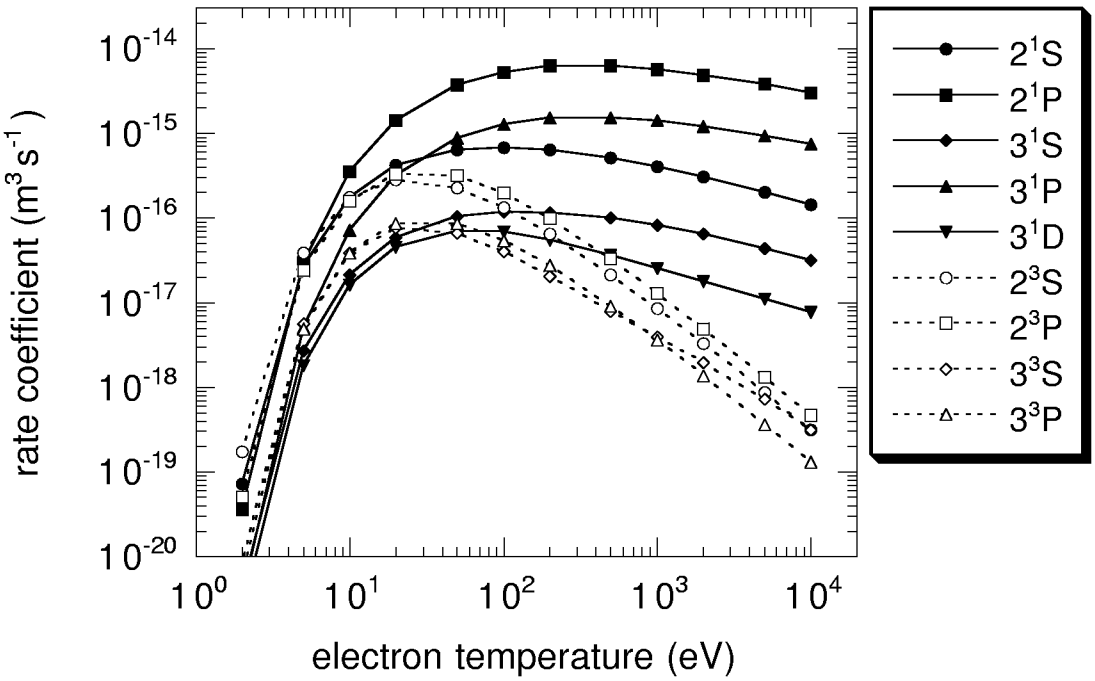

Figure 3.3: Electron temperature dependence of electron impact rate coefficients for excitation out of the He ground state into the two metastable levels and several excited levels [1].

Therefore, injection of neutral helium beams into the plasma should make it possible to determine as plasma parameters not only the electron density, ion density and -temperature, but also the electron temperature.

Extensive modelling has already been done for thermal He beams [33, 36]. Brosda [33] developed a collisional radiative model called HE-BEAM which calculates the population density profiles of a thermal He beam injected into a fusion plasma. At these beam energies the ion collisions can be neglected as the corresponding electron collision cross sections are much larger. For illustration, the cross sections for electron loss and excitation from ground state due to electron and ion impact are shown in figures 3.6 and 3.7. As the slow He beam is fully ionized in the plasma edge, the electron temperature range of interest is from about 1 eV to several 100 eV. Therefore, only electron induced de-/excitation, ionization and spontaneous decay are considered in the model.

As an advantage of the thermal He beam, modelling can be carried out in a rather simple way, but the diagnostic range of plasmas, which is comparable as for fast Li beams, is limited to the plasma edge. The first version of HE-BEAM took into account all levels up to the principal quantum number $n = 4$ (19 levels).

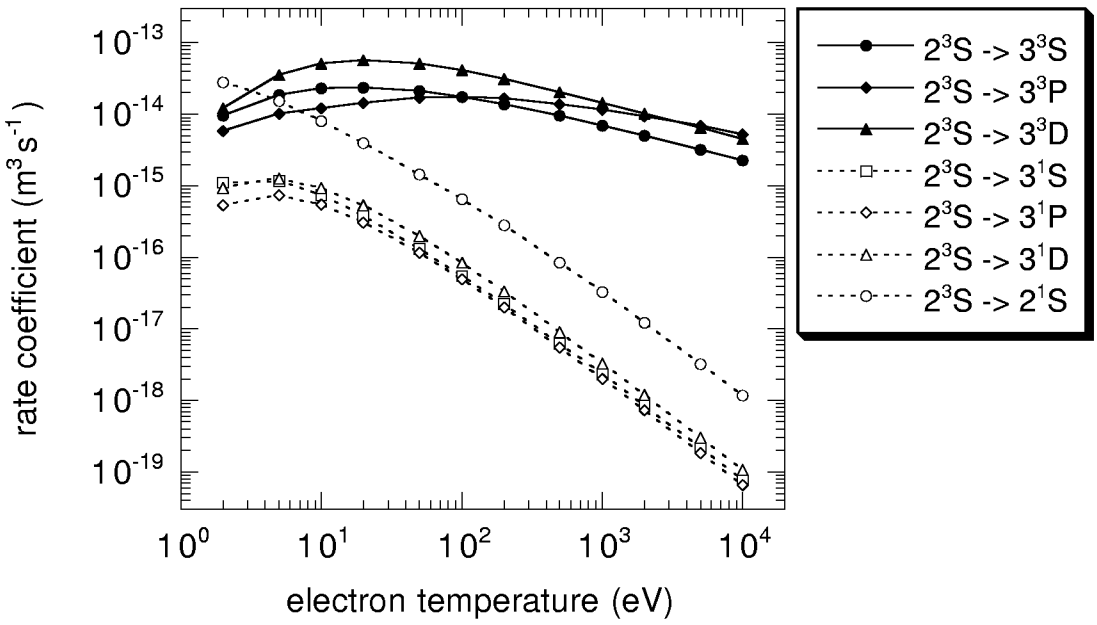

Figure 3.4: Electron temperature dependence of electron impact rate coefficients for excitation out of the metastable triplet He state into several excited levels (n=3) [1].

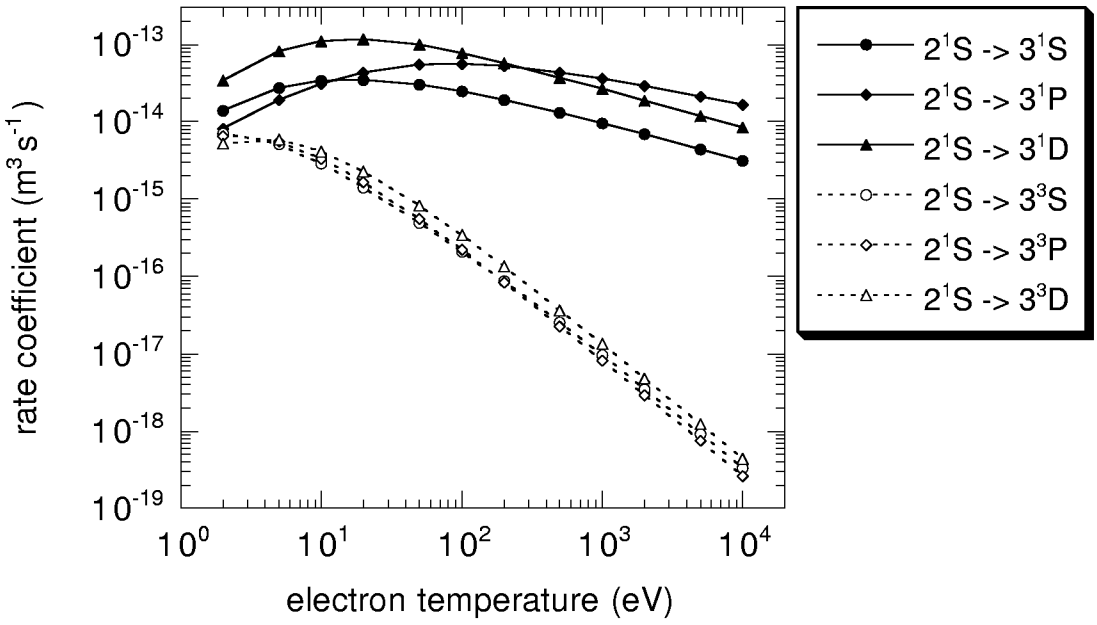

Figure 3.5: Electron temperature dependence of electron impact rate coefficients for excitation out of the metastable singlet He state into several excited levels (n=3) [1].

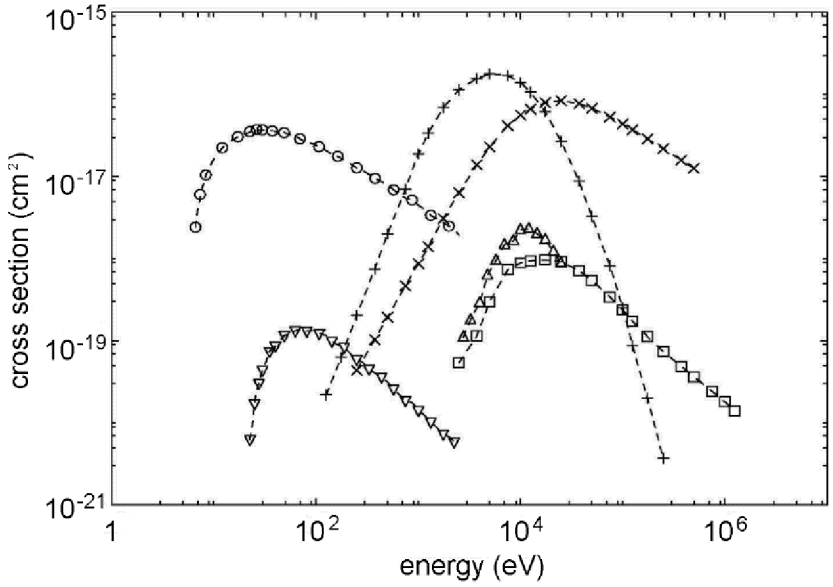

Figure 3.6: Cross sections for electron loss from ground-state He atoms, ∘: single electron impact ionization, △: double electron impact ionization, +: single charge exchange with protons, ×: single proton impact ionization, ▽: proton impact transfer double ionization, □: double proton impact ionization [43].

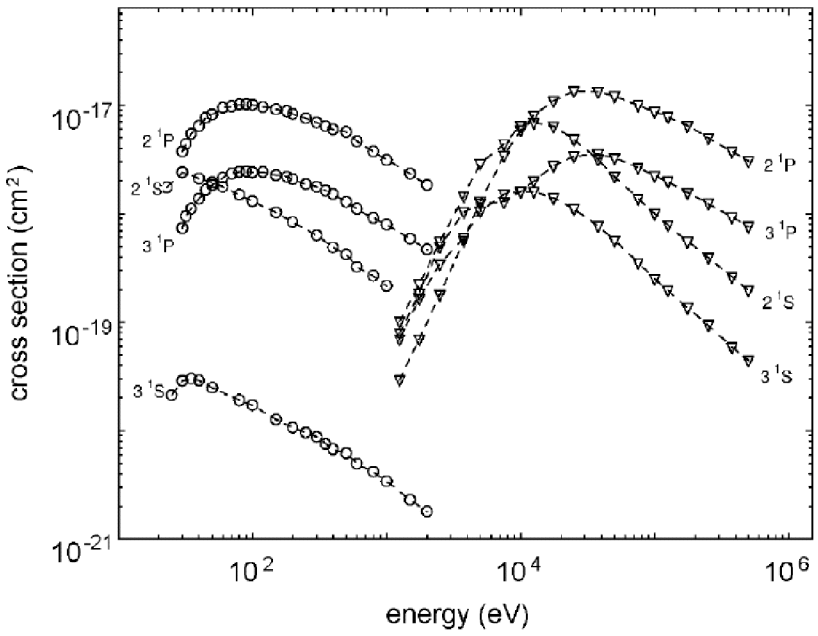

Figure 3.7: Cross sections for electron (∘) and proton (▽) impact excitation from ground-state He atoms into four low excited singlet states [43].

The evaluation routine for determining the plasma parameters from the observed line profiles is based on the fact, that for these slow beam energies the decay length for perturbations in the population of the beam is small compared to the length over which the plasma parameters change significantly. Hence, the excited states are referred to as 'totally relaxed'. From the solution for these totally relaxed excited- and metastable states, line-intensity ratios were determined which are a measure for electron density and -temperature, respectively. All lines considered in the present work except the 505 nm- ($4^1S \rightarrow 2^1P$) and 397 nm- ($4^1P \rightarrow 2^1S$) line were analysed.

Using a line-intensity ratio bears the advantage that no calibration with regard to the geometry of the beam and spectroscopic system has to be performed. The ratios 728 nm/707 nm (singlet/triplet) and 668 nm/728 nm (singlet/singlet) proved to be suitable for determining electron temperature and electron density, respectively. These lines are in the wavelength region (red) where optical spectrometers have large sensitivity and the transmission is almost the same for different wavelengths in usual optical systems. Hence, the system doesn't even have to be calibrated with regard to the frequency sensitivity. Comparison with other diagnostics showed that this model is capable of determining the plasma parameter profiles in the plasma edge of TEXTOR for plasma parameters in the range 10^{18} m$^{-3} < n_e < 10^{19}$ m^{-3} and 20 eV $< T_e <$ 100 eV.

Brix [36] has improved the model by including higher excited states ($n = 5$) and updating the fundamental cross-section data used for modelling. With this the maximum electron density available for diagnostics could be increased to $2{\cdot}10^{19}$ m^{-3} and the maximum electron temperature up to 200 eV. Meanwhile the thermal He beam is used as standard diagnostics at TEXTOR.

With this diagnostic method the plasma parameter profiles are available right from the measurements. This is also a big advantage over Li diagnostics where a time consuming calculation has to be performed. One big problem for the application of thermal He beams at future fusion devices is the beam divergence. At these experimental devices the diagnostic equipment has to be a few meters away from the plasma edge. First experiments at JET and ASDEX Upgrade showed that this problem can be overcome with a fast He beam, see chapter 5 of this thesis. Furthermore, the diagnostics won't be confined to the plasma edge any more.

In contrast to modelling thermal He beams the collisions with ions cannot be neglected for the fast beams considered in this study (several tens of keV), see figures 3.6 and 3.7. The proton-impact excitation cross sections reach values comparable to the electron-impact

excitation for beam energies of about 10 to 30 keV. For a process with a cross section σ the corresponding rate coefficient $\langle \sigma v_r \rangle$ depends on the relative velocity v_r between projectile and target. Although v_r is much larger for collisions between electrons and He atoms than for collisions between protons and He atoms and the ion rate coefficients are accordingly smaller in comparison to the electron rate coefficients, the influence of ion collisions on the beam ionization is still quite substantial. For an illustration, the total loss rate from the He ground state is given in figure 3.8. Note that, due to its dependence on v_r, the ion collision rate coefficients used for simulation in general (see chapter 3.3) depend on the beam energy only (not on the ion temperature), whereas the electron collision rate coefficients depend strongly on the electron temperature, but not on the He beam energy.

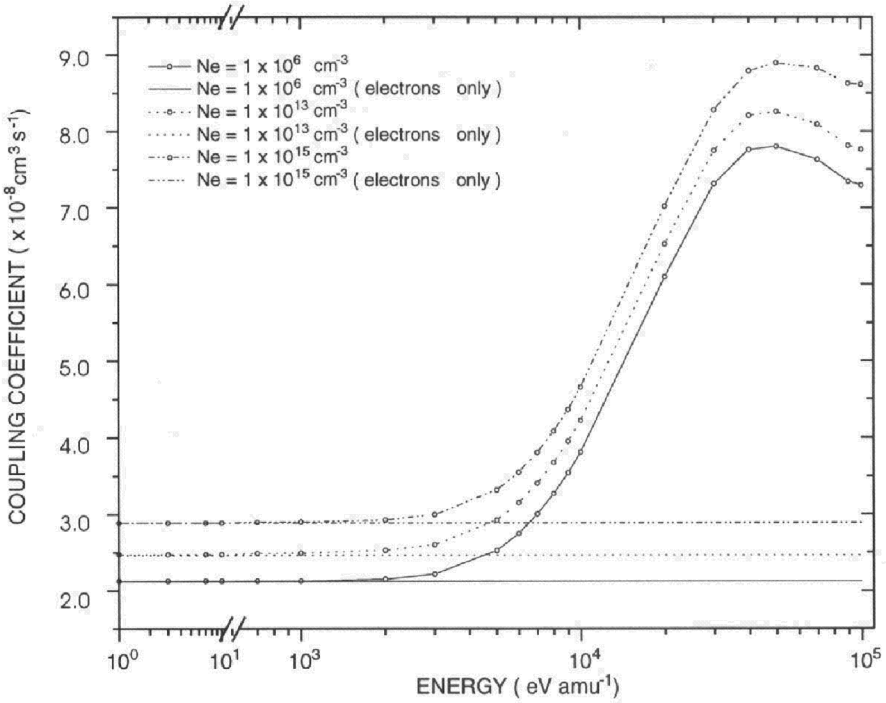

Figure 3.8: Energy dependence of the so-called 'cross-coupling coefficient' describing total loss from ground state He (S_{1^1S}, see chapter 3.3, equation 3.8) in a deuterium plasma with electron temperature of 100 eV for three different electron densities. The constant lines represent the rates when neglecting the influence of the deuterons [43].

In order to investigate the potential of fast He beams as diagnostic tools, which was the aim of this work, we have studied for typical tokamak plasmas (ASDEX Upgrade, JET):

(a) the behaviour of the ground and metastable states in a He beam penetrating the plasma,

(b) line-intensity profiles which could be of interest for diagnostic purposes,

(c) the possibility of determining electron density and -temperature profiles from line-intensity measurements

We also made first predictions on the beam intensity necessary to perform meaningful spectroscopic experiments with fast He beams at fusion devices. The possibility of using fast He beams for charge-exchange spectroscopy is outside the scope of this thesis.

In the following chapters the model used for our He beam simulation is presented. A survey of the fundamental data used for these calculations is given in chapter 3.6. Chapter 3.7 deals with different possibilities of determining the plasma parameter profiles from diagnostic measurements.

3.2 The Collisional-Radiative Model

Plasmas with densities between 10^{17} and 10^{24} m^{-3} are usually described by the so-called 'collisional-radiative model' (cr-model). The principle of the collisional-radiative model is shown in figure 3.9 for a simple atom with a ground state and two excited levels. Also the coronal model for low density plasmas and the high-density model are plotted in figure 3.9.

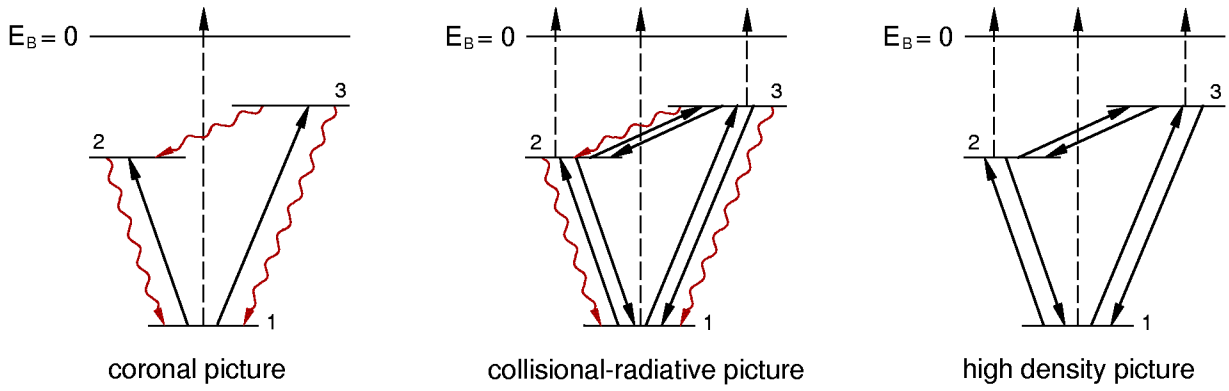

Figure 3.9: The coronal-, collisional-radiative-, and high-density model illustrated for a 3-level atom (ground state and two excited states).

In low density plasmas ($n_{plasma} \leq 10^{17}$ m^{-3}), the probability for spontaneous emission of an excited atom is much higher than for any collisional depopulation process (de-/excitation, ionization). Hence, the only processes considered are collisional excitation and ionization from the ground state and spontaneous emission. For this reason the population density of the excited states is very small in comparison to the ground state population.

In plasmas with higher density (cr-model applies), the collision frequency is higher, which leads to a competition between collisional processes and spontaneous emission. This means that in the cr-model stepwise excitation and ionization from excited states become important.

If the plasma density exceeds 10^{24} m^{-3} (high-density model applies), the collision rates have increased further until spontaneous emission can be neglected, i.e. excited states are depopulated by collisions mainly. In this case the excited states are in local thermodynamic equilibrium with the ground state.

Fusion plasmas are to be described in the cr-model as their plasma densities are in the range of 10^{17} m^{-3} to 10^{22} m^{-3}. The basis of the simulations performed during this work is the cr-model established by the ADAS-(**a**tomic **d**ata and **a**nalysis **s**tructure)[1] group at Strathclyde University in Glasgow. ADAS is a package of tools for assisting with the modelling and analysis of spectral observations of fusion and astrophysical plasmas. It consists of interactive FORTRAN routines driven by an IDL user interface and a collection of fundamental and derived atomic databases. The two ADAS codes used are ADAS311 and ADAS313, which are described in the chapters 3.3 and 3.4. A more detailed description can be found in [43]. The following processes between the beam and the plasma particles have been taken into account:

collisions between He atoms and electrons:	excitation
	de-excitation
	ionization
collisions between He atoms and ions:	excitation
	de-excitation
	ionization
	charge exchange

spontaneous emission from excited He states.

Recombination processes are neglected. The rate for recombination of He ions in the plasma is quite small. Additionally, once a beam atom is ionized it becomes trapped by the magnetic

field. These He ions are quickly removed from the beam and distributed over the respective flux surfaces. Once a particle has been trapped, it is instantly deflected and the probability to become reneutralized inside the beam region with a velocity in the direction of the beam is very small. Hence, the neglection of recombination processes is justified.

In order to solve the population density variation of the He levels of interest we consider the statistical balance equations which represent the rates at which the excited levels of an atom are populated and depopulated. In general these equations are given as:

$$\frac{\partial N_i}{\partial t} + v_b \frac{\partial N_i}{\partial x} = \sum_{j \neq i} \langle \sigma v_r \rangle_{ij,pop.} \, n_t \, N_j - \sum_{j \neq i} \langle \sigma v_r \rangle_{ji,depop.} \, n_t \, N_i + \sum_{j>i} A_{ij} \, N_j - \sum_{j<i} A_{ji} \, N_i \tag{3.1}$$

N_i and N_j denote the population densities of the levels i and j, respectively, v_b the velocity of the projectiles, $\langle \sigma v_r \rangle_{ij,pop.}$ and $\langle \sigma v_r \rangle_{ji,depop.}$ the rate coefficient of the collisional population and depopulation process, n_t the density of the target particles (in this case electrons or ions), and A_{ij} the spontaneous emission coefficient for the emission from level j to level i, respectively. The term $\frac{\partial N_i}{\partial t}$ corresponds to a change in the beam population due to variations in the beam source, but for our calculations this situation will not be considered further,

$$\frac{\partial N_i}{\partial t} = 0. \tag{3.2}$$

Taking into account all processes mentioned above, the rate coefficients for collisionally induced population and depopulation consist of the following expressions:

$$\langle \sigma v_r \rangle_{ij,pop.} = \langle \sigma_{ij,e} v_e \rangle + \langle \sigma_{ij,ion} v_{ion} \rangle, \tag{3.3}$$

$$\langle \sigma v_r \rangle_{ji,depop.} = \langle \sigma_{ji,e} v_e \rangle + \langle \sigma_{ji,ion} v_{ion} \rangle + \langle \sigma_{+i,e} v_e \rangle + \langle \sigma_{+i,ion} v_{ion} \rangle + \langle \sigma_{+i,ce} v_{ion} \rangle. \tag{3.4}$$

v_e and v_p denote the relative velocities between the beam atoms and electrons and protons, respectively. $\sigma_{ji,e}$ stand for the electron induced excitation cross sections from level i to level j, $\sigma_{+i,e}$ is the electron impact ionization cross section and $\sigma_{+i,ce}$ the charge-exchange cross section. The index ion instead of e denotes the corresponding ion impact cross sections.

The population density profile of a He beam penetrating a plasma can be determined by solving these balance equations stepwise, which can be written in matrix form:

$$v_b \frac{dN_i}{dx} = -\sum_j C_{ij} \, N_j. \tag{3.5}$$

C_{ij} is called the collisional-radiative matrix (cr-matrix), which includes all the collisional spontaneous emission contributions mentioned above. Hence, the matrix elements C_{ij} are functions of electron- and ion temperature (T_e, T_i), electron- and ion density (n_e, n_i), and beam energy (E_b):

$$C_{ij} = C_{ij}(T_e, T_i, n_e, n_i, E_b) \tag{3.6}$$

The stepwise solving of the statistical balance equation is being done by the code SCOTTIE developed at IAP, which uses the C_{ij} values calculated from ADAS311 and ADAS313.

3.3 ADAS311

In principle, the statistical balance equations (3.5) could be solved including levels up to an arbitrary principal quantum number n. But with increasing number $\tilde{n}$ of levels treated in non-equilibrium, the equation system gets more and more complex and the solving routine gets slower, as it has to deal with a rectangular matrix of the order $\tilde{n}$. The aim of the first calculations was the prediction of the progression of the He ground state and metastable population and of the expected line intensities in order to assess the favourable metastable content in the initial beam and the minimum beam intensity for first experiments at fusion experiments. For this purpose a simplified version of the cr-model was created by the ADAS-group where all excited states are treated as in equilibrium to ground state 1^1S and the two metastable states 2^1S and 2^3S. Hence, the balance equations were reduced to

$$\begin{aligned}
v_b \frac{dN_{1^1S}}{dx} &= -n_e S_{1^1S} N_{1^1S} + n_e S_{2^1S \to 1^1S} N_{2^1S} + n_e S_{2^3S \to 1^1S} N_{2^3S} \\
v_b \frac{dN_{2^1S}}{dx} &= n_e S_{1^1S \to 2^1S} N_{1^1S} - n_e S_{2^1S} N_{2^1S} + n_e S_{2^3S \to 2^1S} N_{2^3S} \\
v_b \frac{dN_{2^3S}}{dx} &= n_e S_{1^1S \to 2^3S} N_{1^1S} + n_e S_{2^1S \to 2^3S} N_{2^1S} - n_e S_{2^3S} N_{2^3S}
\end{aligned} \tag{3.7}$$

using special condensation techniques [1]. S_{N_i} denotes the total loss from level N_i, $S_{N_i \to N_j}$ stands for the excitation from level N_i to level N_j, including all stepwise processes via excited states. For assessing the progression of the three levels one has to deal only with a (3,3)-matrix. The 9 elements $S_{N_i \to N_j}$ and S_{N_i} of equation (3.8) are called 'generalized radiative coefficients' (GRCs). These GRCs are calculated from ADAS311.

The cross sections, rate coefficients, and spontaneous-emission coefficients for most of the relevant processes involving levels up to principal quantum number $n = 4$ are stored in ADAS (see chapter 3.6), whereas the remaining rate coefficients and those for higher levels are calculated via various approximative methods. The methods available in ADAS311 for the considered processes are:

electron impact excitation:	method of Van Regemorter impact parameter approximation prescription of Percival and Richards
electron impact ionization:	exchange classical impact parameter method of Burgess
ion impact excitation:	semi-empirical formula of Lodge *et al.* impact parameter method two-state approximation of Vainshtein *et al.*
ion impact ionization:	binary encounter formula of Percival and Richards

A detailed description is given in [43]. The first in each list was the method used for our calculations. The corresponding de-excitation cross sections are calculated using the principle of detailed balance.

The levels up to an adjustable level n' are considered as 'nls-resolved', i.e. levels with different principal-, orbital momentum-, and spin quantum numbers are treated as different. Levels with $n > n'$ having the same principal- and spin quantum number are merged ('ns-resolved'). In our calculations n' was chosen to be 5, the maximum principal quantum number was 110. The approximate methods listed above can be used in both pictures, in the nls-resolved picture ion and electron collisions between degenerate levels and electron-driven spin-changing collisions have to be taken into account [83].

In ADAS311 it is assumed that ions and electrons are fully equilibrated, i.e. electron temperature T_e is equal to ion temperature T_i. The velocity of protons can be neglected in comparison to the He beam velocity if

$$T_p[eV] \ll E_{beam}[eV]\sqrt{\frac{m_p}{m_{He}}} = \frac{E_{beam}[eV]}{2}. \tag{3.8}$$

During JET pulses with so called 'internal transport barriers' (modes with very high particle confinement and high temperature and density gradients, see chapter 1.1), maximum ion temperatures of about 35 keV have been measured [14]. Such high ion temperatures cannot

be neglected against beam energies of $\leq$ 80 keV any more. In order to extend the model to cases with such high ion temperatures - which will be of special importance for future plasma regimes - the code has to be modified. However, in the first experiments using fast He beams at JET and ASDEX Upgrade (see chapter 5) the ion temperature was small enough as compared to the beam energy so that the simplification $T_e = T_i$ could be applied.

The input parameters for ADAS311 concerning the plasma and beam are T_e, n_e, and E_b. For each of these parameters up to 25 values can be chosen and the code then scans through these parameters. The scans are a mixture of one- and two-dimensional scans relative to the chosen reference values T_e^{ref}, n_e^{ref}, and E_b^{ref}. In the first version of ADAS311 the output coefficients for all combinations of n_e and E_b at T_e^{ref} are calculated (two-dimensional scan in the (n_e,E_b)-plane), and then the output coefficients for the one-dimensional T_e scan at the reference values n_e^{ref} and E_b^{ref} are generated. The GRCs can be calculated for each fully stripped ion species from He^{2+} up to Ne^{10+}.

These GRCs can then be used to calculate the development of the population densities of the three non-equilibrium levels. The population densities of the excited states can be calculated by solving the corresponding balance relations (equation (3.1), $\frac{dN_i}{dt} = \frac{dN_i}{dx} = 0$) for the given parameters T_e, n_e, and E_b. Every level has a contribution from each of the 3 non-equilibrium states. ADAS311 creates special excitation coefficients [43] for the subsequent calculation of the excited population contributions performed by ADAS313 (see chapter 3.4). The output file of ADAS311 is stored in the ADAS data format adf26 [1]. It has a typical size of 7 Mb. To assist in extracting the coefficients needed for the following calculations, an interactive program (ADAS313) has been developed (see the following subchapter 3.4).

3.4 ADAS313

The line intensity I_{ji} (photons per $m^{-3}s^{-1}$) for emission from level i to level j depends on the population density N_i (m^{-3}) and the spontaneous emission coefficient A_{ji} (s^{-1}):

$$I_{ji}(T_e, n_e, E_b, N_{1^1S}, N_{2^1S}, N_{2^3S}) = N_i(T_e, n_e, E_b, N_{1^1S}, N_{2^1S}, N_{2^3S})\, A_{ji}. \tag{3.9}$$

Based on excitation coefficients generated by ADAS311, the code ADAS313 calculates for each excited level N_i of interest the so called "effective beam emission coefficients" (EECs) $E_{ji}(T_e, n_e, E_b, N_k)$ for each non-equilibrium level N_k at given values of T_e, n_e, and E_b:

$$E_{ji}(T_e, n_e, E_b, N_k) = \frac{A_{ji}\, N_i(T_e, n_e, E_b, N_k)}{n_e\, N_k(T_e, n_e, E_b)} \tag{3.10}$$

Hence, the line intensity I_{ji} can be written as

$$I_{ji} = \sum_{k=1}^{3} (E_{ji}\, n_e\, N_k) \tag{3.11}$$

ADAS313 generates the EECs for all optical emission lines of interest listed in table 3.1 and stores them in adf22 type files. As mentioned earlier, ADAS313 can also extract the GRCs, which are stored in adf21 type files. The structure of both file formats adf21 and adf22 is (like in the underlying adf26 files) the mixed two-dimensional(n_e,E_b)/one-dimensional(T_e) scan.

transition	wavelength
$4^1P \rightarrow 2^1S$	396.5 nm
$4^1D \rightarrow 2^1P$	492.2 nm
$3^1P \rightarrow 2^1S$	501.6 nm
$4^1S \rightarrow 2^1P$	504.8 nm
$3^1D \rightarrow 2^1P$	667.8 nm
$3^1S \rightarrow 2^1P$	728.1 nm
$3^3P \rightarrow 2^3S$	388.9 nm
$4^3D \rightarrow 2^3P$	447.1 nm
$4^3S \rightarrow 2^3P$	471.3 nm
$3^3D \rightarrow 2^3P$	587.6 nm
$3^3S \rightarrow 2^3P$	706.5 nm

Table 3.1: Optical lines of interest: Transitions and corresponding wavelengths.

ADAS311 and ADAS313 can also be run in a mode where ion collisions are neglected. This opens a way to estimate the influence of the ions on the beam atoms.

The first simulations have been carried out for pure electron-/deuteron plasmas ($n_e = n_p$, $Z_{eff} = 1$) with impurities neglected.

The GRCs enable for calculation of ground state and metastable level populations of the He beam on its way into the plasma for given T_e- and n_e profiles and given E_b. From these results the line intensities can be determined at each point on the beam path using the EECs. This is been done by the code SCOTTIE developed at IAP.

3.5 SCOTTIE

The code SCOTTIE [84] generates the GRCs and EECs for the plasma parameter combinations (n_e, T_e, E_b) needed for the model calculations. Then it determines the population progression of the ground state and the two metastable levels of the He beam (E_b) and the resulting line-intensity profiles for the optical lines of interest (see table 3.1) for given T_e- and n_e profiles by using the GRCs and EECs as provided by ADAS313. The code requires the following input parameters:

beam parameters:	initial population densities (1^1S, 2^1S, 2^3S)
	equivalent beam current
	beam energy
	beam diameter
plasma parameters:	T_e profiles
	n_e profiles
model parameters:	path length
	number of steps for calculation.

The code exists in two forms, one with exponentially increasing T_e- and n_e profiles with distance x and a second one with the T_e- and n_e profiles considered as linearly dependent on x. The first one is used for the calculations in the scrape-off layer, i.e. the region outside the separatrix (last closed flux surface) where the density and temperature values decay rapidly with decay lengths of about 1 cm to 3 cm. The input parameters used are the plasma values at the separatrix (T_e^S, n_e^S) and the corresponding decay lengths (λ_T, λ_n). The second version is applied for the region inside the separatrix where the plasma is divided into sections with plasma parameters treated as linearly varying with distance x. Here the input parameters are the initial and final T_e and n_e, respectively.

After reading the input file, SCOTTIE calculates the (T_e,n_e)-pairs for each calculation step. As in general the GRCs and EECs needed for one calculation step do not explicitly appear in the corresponding ADAS file, SCOTTIE has to interpolate the GRCs and EECs in the (n_e, E_b) plane and then to interpolate in the T_e dimension. The interpolation in T_e- and E_b direction has been done linearly, whereas the interpolation in the n_e direction has been performed logarithmically [43]. Afterwards the change in the population densities of 1^1S, 2^1S, and 2^3S is determined by solving equation 3.8 stepwise. Then at each calculation step

the intensity of each line of interest is calculated using equation 3.11. The single results are stored in tables prepared for plotting in spread sheets.

3.6 Fundamental Data

There are three databases in ADAS which contain the fundamental data relevant for the calculations of the He beam:

helike_kvi97#he0.dat:	electron impact excitation
ionelec_szd#he.dat:	electron impact ionization
he.dat:	ion impact reactions

Each of this data is stored in a different data format ('adf': ADAS data format [1]).

3.6.1 Electron Impact Excitation Data

The fundamental data is stored in an adf04 file called 'helike_kvi97#he0.dat' (current location in ADAS: adf04\helike\) as effective collision strengths Y_{ij}, which are dimensionless parameters defined by

$$\langle \sigma v_r \rangle_{ji} = \left(\frac{2\sqrt{\pi}\alpha c a_o^2}{g_i} \right)^{\left(-\frac{E_j - E_i}{kT_e}\right)} \sqrt{\frac{E_{Ry}}{kT_e}} Y_{ij}, \tag{3.12}$$

where i stands for the lower initial level and j for the higher final level. E_i and E_j are the corresponding binding energies, α denotes the fine-structure constant ($\alpha = 7.297 \cdot 10^{-3}$), a_o the Bohr radius ($a_o = 5.29 \cdot 10^{-11}$ m), g_i the statistical weight of level i, and E_{Ry} the Rydberg energy ($E_{Ry} = 13.6$ eV). The collision strengths depend weakly on T_e. They are given for the transitions shown in tab. 3.2.

Most of the data is taken from a compilation of deHeer [85] from 1995. The data can be interrogated with ADAS201, which produces the corresponding rate coefficients for a chosen electron temperature region. The file also includes spontaneous emission coefficients.

↓i j→	1	3	5	7	10	11	13	16	18	19	2	4	6	8	9	12	14	15	17
1 (1^1S)	–	•	•	•	•	•	•	•	•	•	•	•	•	•	•	•	•	•	•
3 (2^1S)	*	–	•	•	•	•	•	•	•	•	*	•	•	•	•	•	•	•	•
5 (2^1P)	*	*	–	•	•	o	•	•	o	o	*	*	o	o	o	o	o	o	o
7 (3^1S)	*	*	*	–	o	•	o	o	o	•	*	o	o	o	o	o	o	o	o
10 (3^1D)	*	*	*	o	–	•	o	o	•	•	*	o	o	o	o	o	o	o	o
11 (3^1P)	*	*	o	*	*	–	•	•	o	o	*	o	o	o	o	o	o	o	o
13 (4^1S)	*	*	*	o	o	*	–	o	o	•	*	o	o	o	o	o	o	o	o
16 (4^1D)	*	*	*	o	o	*	o	–	•	•	*	o	o	o	o	o	o	o	o
18 (4^1F)	*	*	o	o	*	o	*	*	–	o	*	o	o	o	o	o	o	o	o
19 (4^1P)	*	*	o	*	*	o	*	*	o	–	*	o	o	o	o	o	o	o	o
2 (2^3S)	*	•	•	•	•	•	•	•	•	•	–	•	•	•	•	•	•	•	•
4 (2^3P)	*	*	•	o	o	o	o	o	o	o	*	–	•	o	•	•	o	•	o
6 (3^3S)	*	*	o	o	o	o	o	o	o	o	*	*	–	•	o	o	•	o	o
8 (3^3P)	*	*	o	o	o	o	o	o	o	o	*	o	*	–	•	•	o	•	o
9 (3^3D)	*	*	o	o	o	o	o	o	o	o	*	*	o	*	–	o	•	o	•
12 (4^3S)	*	*	o	o	o	o	o	o	o	o	*	o	o	*	o	–	•	o	o
14 (4^3P)	*	*	o	o	o	o	o	o	o	o	*	o	*	o	*	*	–	•	o
15 (4^3D)	*	*	o	o	o	o	o	o	o	o	*	*	o	*	o	o	*	–	•
17 (4^3F)	*	*	o	o	o	o	o	o	o	o	*	o	o	o	*	o	o	*	–

Table 3.2: Electron impact excitation from level i to level j for the 19 lowest HeI levels ($n \leq 4$). Fundamental data contained in ADAS is marked with •, derived deexcitation data denoted with $*$ (see chapter 3.3), and $\circ$ denotes data not available from ADAS.

3.6.2 Electron Impact Ionization Data

This data is stored in an adf07 file called 'ionelec_szd#he.dat' (current location in ADAS: adf07\ionelec\) as Maxwell-averaged rate coefficients for the following processes:

$$\mathrm{He}(1^1\mathrm{S}) + \mathrm{e}^- \rightarrow \mathrm{He}^+ + 2\mathrm{e}^-$$
$$\mathrm{He}(2^3\mathrm{S}) + \mathrm{e}^- \rightarrow \mathrm{He}^+ + 2\mathrm{e}^-$$
$$\mathrm{He}(2^1\mathrm{S}) + \mathrm{e}^- \rightarrow \mathrm{He}^+ + 2\mathrm{e}^-$$

The rate coefficients for the ground state are taken from Bell *et al.* [86], those for the metastable levels from Fujimoto [34]. The ADAS interrogating routine is ADAS502.

3.6.3 Ion Collision Data

This data is stored as cross sections in adf02 file called 'he.dat' (current location in ADAS: adf02\ionatom\). It contains cross sections for the following processes:

single- and double ionization:

$$He(1^1S) + A^{Z+} \rightarrow He^{+} + A^{Z+} + e^{-}$$
$$He(2^3S) + A^{Z+} \rightarrow He^{+} + A^{Z+} + e^{-}$$
$$He(1^1S) + A^{Z+} \rightarrow He^{2+} + A^{Z+} + 2e^{-}$$

single- and double charge exchange:

$$He(1^1S) + A^{Z+} \rightarrow He^{+} + A^{(Z-1)+*}$$
$$He(2^3S) + A^{Z+} \rightarrow He^{+} + A^{(Z-1)+*}$$
$$He(1^1S) + A^{Z+} \rightarrow He^{2+} + A^{(Z-2)+*}$$

transfer double ionization:

$$He(1^1S) + A^{Z+} \rightarrow He^{2+} + A^{(Z-1)+} + e^{-}$$

excitation:

$$He(1^1S) + H^{+} \rightarrow He^{*} + H^{+}$$

He^* ... $He(2^1S)$, $He(3^1S)$, $He(4^1S)$, $He(2^1P)$ $He(3^1P)$, $He(4^1P)$, $He(3^1D)$, and $He(4^1D)$

The ionization- and charge-exchange cross sections are available for the following ion species A^{Z+}:

$$H^{+}, He^{2+}, Be^{4+}, C^{6+}, \text{and } O^{8+}.$$

The fundamental data for B^{5+}, N^{7+}, and Ne^{10+} is stored as 'total stopping' cross sections only, i.e. the sum of single and double ionisation-, charge-exchange-, and transfer double ionisation cross sections. The data is based on a compilation of Summers [1] from 1990 and 1991, and it can be interrogated by ADAS302.

3.7 Application of He Beams for Plasma Diagnostics

In the present work the potential of He fast beams as diagnostic tools is investigated by modelling the beam emission of a helium beam penetrating into a fusion plasma using assumed plasma temperature- and density profiles. For future application of fast He beams for plasma diagnostics, the inverse procedure has to be applied, i.e. plasma parameters have to be deduced from He emission profiles. Several techniques have been considered as candidates for achieving this goal, e.g.:

Line-intensity ratios,
Inverting the balance equations,
Iterative method, and
Neural networks.

Line-intensity ratios

As already mentioned in chapter 1.2.8.3, this method is used as a standard technique for deduction of temperature- and density profiles from emission of thermal He beams. This is possible as the ratios of singlet/singlet emission of these slow beams (e.g. 668 nm/728 nm) are dominated by plasma density but quite insensitive to temperature, whereas singlet/triplet ratios (e.g. 728 nm/707 nm) are dominated by plasma temperature and quite insensitive to density. As ascertained by Brix [92] and also verified in our sensitivity study (chapter 4.2), the He emission and line-intensity ratios are quite sensitive to the metastable fraction in the beam. A thermal He beam with initially no metastable fraction quickly reaches equilibrium with a very small metastable fraction while penetrating the plasma. In contrast, a fast He beam has an initial metastable fraction of 3% or more from its charge-exchange products. While penetrating the plasma this metastable fraction is being rearranged, which means that the relation between intensity ratios and electron temperature changes along the penetration path. Furthermore, the local population density of the triplet states is dominated by the collision frequency and the line ratio of singlet- and triplet lines becomes sensitive to density as well as temperature.

Inverting the balance equations

This is the standard technique in Li-beam diagnostics for deduction of electron density profiles (see chapter 3.1). Inverting the balance equations of the He beam is not as trivial

as in the Li case since not only one but 3 non-equilibrium levels have to be considered. Furthermore, the Li diagnostics deals with only one plasma parameter, i.e. the electron density, as the observed Li emission is almost independent of the electron temperature. Nevertheless, an algorithm as used for Li beams could be used in first approximation for calculating a density profile using a He-beam emission line which is only weakly sensitive to temperature.

Iterative method

From the beam-emission profile of a HeI line which is mainly sensitive to density, a first approximation of a plasma density profile can be calculated, assuming a reasonable temperature profile. The first approximation of the temperature profile could be obtained from the line-average temperature which is available in real time from other diagnostics. Due to the profile stiffness observed in various Tokamak experiments [88] this first approximation should already be quite accurate in most cases. Having calculated a density profile, the second approximation of the temperature profile can be calculated from the emission profile of a line with reasonable sensitivity to temperature, using the first approximation of the density profile. This procedure can now be iterated. As some line intensities have a high sensitivity to density and only weak sensitivity to temperature, it can be expected that this procedure will quickly converge to a selfconsistent solution.

Neural networks

Neural networks could be used to determine temperature- and density profiles rather quickly. Dragosics [87] investigated such neural networks in view of the application for fast He beam diagnostics. In these first studies the potential of neural networks was tested with Li beam diagnostic emission profiles as the results could be easily cross-checked with results from the inversion method. By training the neural networks with Li-emission profiles and the corresponding density profiles, it was possible to reconstruct the plasma parameter profiles from given emission profiles. A reconstruction accuracy of 6% and a calculation duration of less than 3 ms could be reached, which would enable for real-time evaluation. A disadvantage of this method is the fact that solutions for emission profiles are not reliable in case these profiles are not comparable with any of the training profiles. For the application in He-beam diagnostics not only one but two emission profiles are expected to be needed as input: One profile should be predominantly sensitive to temperature and the other one predominantly sensitive to density. So far it has not been verified whether this method will lead to a selfconsistent solution in the case of He-beam diagnostics.